

Iterative synthesis of monodisperse pendants for making comb-like polyurethanes



Chien-Hsin Wu^a, Yu-Ching Chen^a, Shenghong A. Dai^b, Su-Chen Chen^c,
Shih-Huang Tung^{a, **}, Rong-Ho Lee^{b, ***}, Wen-Chiung Su^d, Ru-Jong Jeng^{a, *}

^a Institute of Polymer Science and Engineering, National Taiwan University, Taipei 106, Taiwan

^b Department of Chemical Engineering, National Chung Hsing University, Taichung 402, Taiwan

^c Department of Energy and Materials Technology, Hsiuping University of Science and Technology, Taichung 412, Taiwan

^d Chung-Shan Institute of Technology, Lungtan, Taoyuan 325, Taiwan

ARTICLE INFO

Article history:

Received 28 February 2017

Received in revised form

1 May 2017

Accepted 6 May 2017

Available online 6 May 2017

Keywords:

Iterative synthesis

Dendrons

Polyurethanes

Shape memory materials

ABSTRACT

Polyurethanes grafted with well-defined polar pendants were synthesized and investigated. A series of linear and dendritic poly(urea/malonamide)s with uniform chain length were first prepared from an iterative synthesis route, which is based on a dual-functional building block, 4-isocyanate-4-(3,3-dimethyl-2,4-dioxo-azetidinediphenyl methane (IDD). Moreover, side chain polyurethanes (SPUs) bearing azetidine-2,4-dione functional groups were prepared from one pot reaction for following post-functionalization of poly(urea/malonamide)s when IDD-diols were added to polyurethane prepolymers as chain extenders. Subsequently, the azetidine-2,4-dione functional groups on the SPUs underwent addition reactions with amino functional group containing dendritic or linear poly(urea/malonamide)s under mild condition, without the need of catalyst and protection/deprotection procedure to achieve polyurethanes grafted with well-defined pendants. Mechanical properties of these comb-like polyurethanes strongly depend on the architecture and the molecular length of poly(urea/malonamide) pendants, which could be adjusted by the grafting fractions of the dendritic or linear poly(urea/malonamide)s with various generations. These poly(urea/malonamide) pendants provided strong hydrogen bonding interactions to achieve physical crosslinking effects in the polyurethanes. Consequently, the polyurethanes with improved mechanical properties and sustained phase transition exhibit shape memory properties.

© 2017 Elsevier Ltd. All rights reserved.

1. Introduction

Segmented polyurethanes (PUs) are copolymers composed of hard-segment and soft-segment (HS and SS) in an alternative manner. Phase separation between HS and SS are governed by the choice of isocyanates and polyols raw materials, forming a variety of properties for end-use applications [1,2]. Many studies relating to the hard- and soft-phase segregation phenomenon of PUs have been reported [3,4]. Apart from that, several studies have revealed the micro phase separation of comb-like PUs. The micro phase

separation and functionality of comb-like PUs are strongly dependent on the type and length of grafted pendants [5–19]. Therefore, the investigation of the incorporating pendants is of great interest in this field. However, most of the grafted pendants are limited to either small molecules or nonpolar segments with linear architecture. Stirna et al. performed a reaction between diisocyanates and urethane groups on the PU chains, which resulted in the formation of allophanate branching units and isocyanate-containing pendants [17]. Subsequently, flexible side chains were introduced to PUs via isocyanate-containing pendants. These PUs exhibited improved elasticity and solubility. However, the formation of allophanate linkages had to be carried out at temperatures higher than 150 °C, and it is difficult to monitor the precision of reaction. Moreover, Eisenbach et al. have reported the pendants preparation from harsh reagents and physical properties of PUs comprising uniform urethane-based linear side chains [20–22], demonstrating that supramolecular

* Corresponding author.

** Corresponding author.

*** Corresponding author.

E-mail addresses: shtung@ntu.edu.tw (S.-H. Tung), rhl@nchu.edu.tw (R.-H. Lee), rujung@ntu.edu.tw (R.-J. Jeng).

structures could be created via macromolecular architecture.

Iterative pathway is a useful methodology in organic chemistry to the synthesis of monodisperse oligomers or polymer precursors [23]. Well-defined nanoarchitectures based on this specific preparation would advance polymer synthesis further [24–26]. Through the similar reaction sequence, dendrimers or linear supramolecules with repeated building blocks has been developed [27]. Recently, we used a methylene di-*para*-phenyl isocyanate (MDI) based selective building block, 4-isocyanate-4-(3,3-dimethyl-2,4-dioxazetidine)diphenyl methane (IDD) with dual functionalities, to repetitively synthesize a series of poly(urea/malonamide) structures without resorting to protection and deprotection process [26,28–31]. The dendritic side chain and end-capped PUs was found to show strong intermolecular association due to the presence of hydrogen bond-rich dendritic structures [32–34]. By incorporation of the dendritic structures with peripheral long hydrophobic alkyl chains, the microphase separation in the side chains led to an increase of the possibility to form hydrogen bonds in the urea/malonamide domains. Consequently, the hydrogen bonding reinforced hard segments of side chain dendritic PUs greatly enhanced the mechanical properties. In addition, several linear chain extenders with uniform chain lengths were synthesized based on the dual functional building block IDD [35,36]. The increase in the number of hydrogen bonding sites resulted in a higher physical cross-linking degree in the HS domains, leading to supramolecular PUs.

Based on the above results, it is important to establish the structure–property relationships of PUs in terms of the impacts of different pendants with precise chain lengths on the thermal and mechanical properties via efficient and iterative syntheses. In this study, we investigated the syntheses and mechanical properties of PUs grafted with polar pendants of various architectures and chain lengths. First, a series of uniform-length pendants with linear or dendritic architecture were synthesized iteratively in absence of catalyst, including the linear architecture of various generations (LGs), LG0.5, LG1.0, LG1.5, LG2.0, LG2.5, LG3.0, and LG3.5, and the

dendritic architecture of various generation (DGs), DG0.5, DG1.0, DG1.5, DG2.0, and DG2.5. Subsequently, reactive side chain polyurethanes (SPUs) were prepared from the same batch for following post-functionalization of well-defined polar pendants. This strategy aims at limiting the variation effects of the molecular weight and polydispersity on the properties of PUs [37,38]. In our previous works [32–34], intensive physical crosslinking interactions were achieved by the incorporation of hydrogen bond-rich poly(urea/malonamide)s into PUs. Thus, we also investigated the thermal mechanical properties along with shape memory behavior. The results indicate that these polar pendants with well-defined structures have a great impact on shape memory properties.

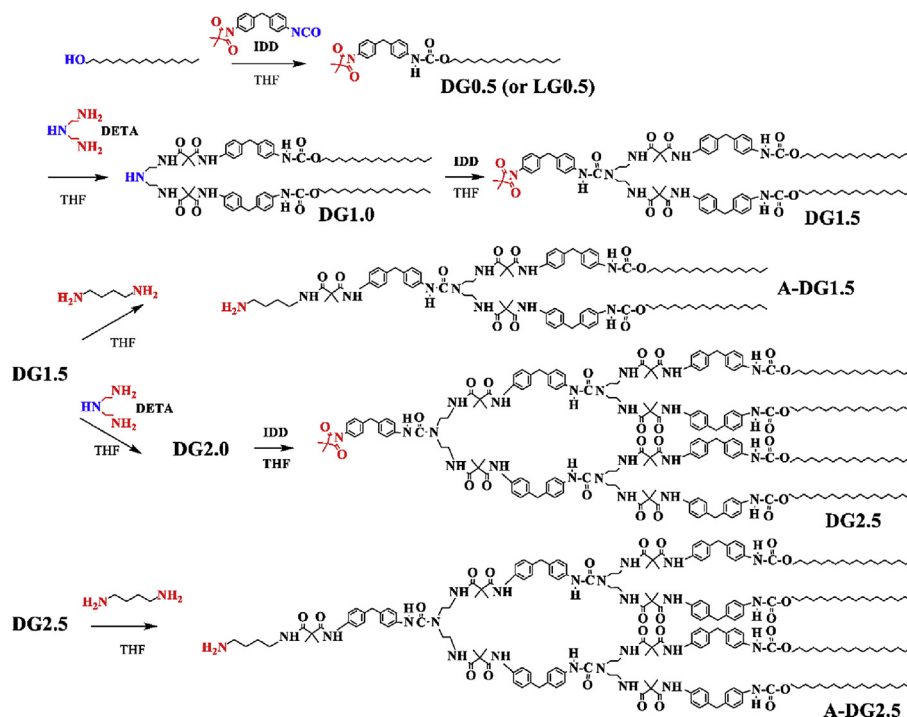
2. Experimental

2.1. Materials

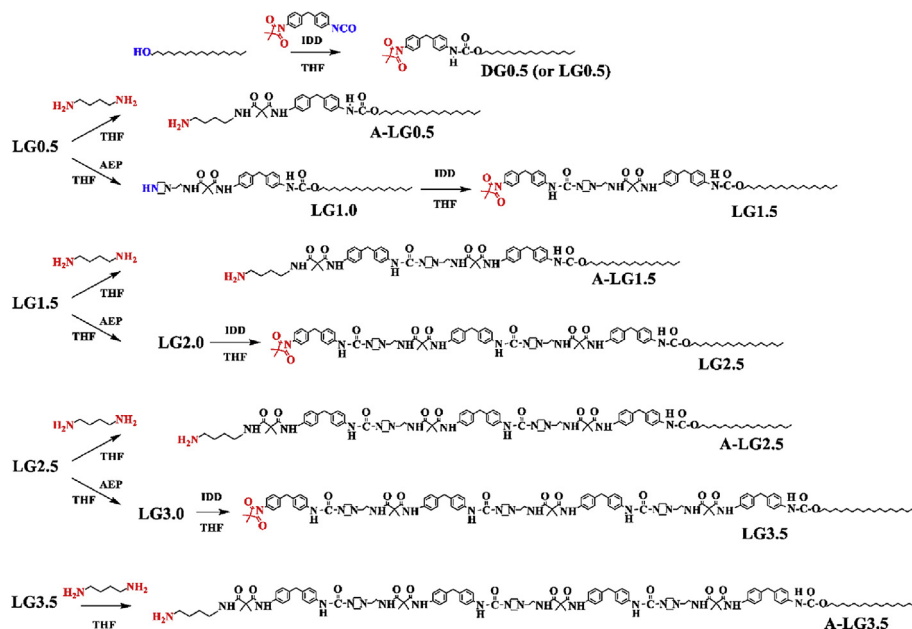
Methylene di-*p*-phenyl diisocyanate (MDI), isobutryl chloride, triethylamine (TEA), stearyl alcohol, diethylene glycol (DEG), diethanolamine (DEA), 1,6-diaminohexane, catalyst dibutyltin dilaurate (T-12), and 1-(2-aminoethyl)piperazine (AEP), 1,4-diaminobutane, and 1,2-ethylenediamine (EDA), were all reagent grade and used as received from Aldrich, Arcos, Showa and Tedia. Xylene, tetrahydrofuran (THF), dimethylformamide (DMF), acetone, and cyclohexane were distilled under reduced pressure over CaH₂ and stored over 4 molecular sieves. Polycaprolactone diol (PCL 2303, Mn = 3000), purchased from Perstorp Specialty Chemicals Company, Sweden, which was dried and degassed at 80 °C, 1–2 mm Hg for 4 h before use.

2.2. Synthesis of dendritic (DGs) and linear (LGs) hydrogen bond-rich urea/malonamide

The synthesis routes are shown in Scheme 1 (DGs) and Scheme 2 (LGs). The detailed synthesis procedures of DGs (DG0.5, DG1.0, DG1.5, DG2.0 and DG2.5) based on building block 4-isocyanate-4-



Scheme 1. Preparation of dendritic pendants.



Scheme 2. Preparation of linear pendants.

(3,3-dimethyl-2,4-dioxo-azetidine)diphenyl methane (IDD) have been reported in the previous literature [32]. Moreover, the general procedure for making linear poly(urea/malonamide), LGs (LG0.5, LG1.0, LG1.5, LG2.0, LG2.5, LG3.0 and LG3.5), were described as below. It is noted that the chemical structure of LG0.5 are LG0.5 are the same.

2.2.1. LG1.0

A solution of AEP (1.64 g, 12.71 mmol) in dry DMF (5 mL) was added slowly to a solution of LG0.5 (5 g, 8.47 mmol) in dry DMF (30 mL) under dry N₂ at 60 °C. After 2 h, all of LG0.5 had been consumed, the mixture was then poured into water (150 mL) and stirred for several minutes. The precipitate was purified through two cycles of dissolving in DMF and precipitating from water. Via drying under vacuum at 60 °C for 48 h, LG1.0 (5.5 g, 90%) was obtained as white powder. FT-IR (KBr): 3321 cm⁻¹ (NH), 1704 cm⁻¹ (C=O, urethane), 1650 cm⁻¹ (C=O, malonamide); ¹H NMR (Chloroform-d): δ(ppm) = 0.86 (t, 3H, -CH₃), 1.23 (m, 30H, -CH₂), 1.53 (s, 6H, -CH₃), 1.64 (m, 2H, -CH₂), 2.3–2.46 (m, 6H, NH-(CH₂-CH₂)₂-N; N-CH₂-CH₂-NHCO), 2.81 (t, 4H, NH-(CH₂-CH₂)₂-), 3.32 (t, 2H, CONH-CH₂), 3.86 (s, 2H, Ar-CH₂-Ar), 4.13 (t, 2H, NHCOO-CH₂), 7.05–7.44 (m, 8H, Ar-H); Anal. Calcd for C₄₃H₆₉N₅O₄: Calcd. C, 71.73; H, 9.66; N, 9.73; Found C, 71.4; H, 9.70; N, 9.15; MS: *m/z* (ESI) 720 [M⁺]. GPC (THF): polydispersity = 1.01, Mw = 1198 g/mol, Mn = 1152 g/mol.

2.2.2. LG1.5

A solution of IDD (3.4 g, 10.42 mmol) in dry THF (5 mL) was added slowly to a solution of LG1.0 (5 g, 6.94 mmol) in dry THF (45 mL) under dry N₂ at 60 °C. After 4 h, all of LG1.0 had been consumed. The solvent was evaporated and the product was purified through two cycles of dissolving in THF and precipitating from methanol. Via drying under vacuum at 60 °C for 48 h, LG1.5 (5.8 g, 80%) were obtained as white powder. FT-IR (KBr): 3338 cm⁻¹ (NH), 1855, 1735 cm⁻¹ (C=O, azetidine-2,4-dione), 1704 cm⁻¹ (C=O, urethane), 1650 cm⁻¹ (C=O, malonamide); ¹H NMR (DMSO-d₆): δ(ppm) = 0.79 (t, 3H, -CH₃), 1.23 (m, 30H, -CH₂), 1.33 (s, 12H, -CH₃), 1.53 (m, 2H, -CH₂), 2.3–2.46 (m, 6H, N-(CH₂-CH₂)₂-N-CH₂-), 3.16–3.39 (t, 6H, CONH-CH₂-CH₂), 3.73 (s, 2H, Ar-CH₂-Ar), 3.81 (s,

2H, Ar-CH₂-Ar), 3.98 (t, 2H, NHCOO-CH₂), 7.98–7.56 (m, 16H, Ar-H); Anal. Calcd for C₆₂H₈₅N₇O₇: Calcd. C, 71.58; H, 8.23; N, 9.42; Found C, 68.9; H, 7.55; N, 11.52; MS: *m/z* (ESI) 1040 [M⁺]. GPC (THF): polydispersity = 1.01, Mw = 1929 g/mol, Mn = 1893 g/mol.

2.2.3. LG2.0

A solution of AEP (0.93 g, 7.21 mmol) in dry DMF (10 mL) was added slowly to a solution of LG1.5 (5 g, 4.81 mmol) in dry DMF (40 mL) under dry N₂ at 60 °C. After 4 h, all of LG1.5 had been consumed, the mixture was then poured into water (150 mL) and stirred for several minutes. The precipitate was purified through two cycles of dissolving in DMF and precipitating from water. Via drying under vacuum at 60 °C for 48 h, LG2.0 (5.1 g, 90%) was obtained as white powder. FT-IR (KBr): 3328 cm⁻¹ (NH), 1704 cm⁻¹ (C=O, urethane), 1642 cm⁻¹ (C=O, malonamide); ¹H NMR (Chloroform-d): δ(ppm) = 0.85 (t, 3H, -CH₃), 1.23 (m, 30H, -CH₂), 1.61 (s, 12H, -CH₃), 1.81 (m, 2H, -CH₂), 2.3–2.36 (m, 12H, NH-(CH₂-CH₂)₂-N-CH₂-), 2.81 (t, 4H, NH-(CH₂-CH₂)₂-), 3.17–3.39 (m, 8H, CH₂-CH₂-NHCO; N-(CH₂-CH₂)₂-N-CH₂-), 3.84 (s, 4H, Ar-CH₂-Ar), 4.1 (t, 2H, NHCOO-CH₂), 7–7.5 (m, 16H, Ar-H); Anal. Calcd for C₆₈H₁₀₀N₁₀O₇: Calcd. C, 69.83; H, 8.62; N, 11.98; Found C, 68.9; H, 7.55; N, 11.52; MS: *m/z* (ESI) 1169 [M⁺]. GPC (THF): polydispersity = 1.01, Mw = 2140 g/mol, Mn = 2117 g/mol.

2.2.4. LG2.5

A solution of IDD (2.05 g, 6.41 mmol) in dry THF (5 mL) was added slowly to a solution of LG2.0 (5 g, 4.28 mmol) in dry THF (45 mL) under dry N₂ at 60 °C. After 6 h, all of LG2.0 had been consumed. The solvent was evaporated and the product was purified through two cycles of dissolving in THF and precipitating from methanol. Via drying under vacuum at 60 °C for 48 h, LG2.5 (5.1 g, 80%) was obtained as white powder. FT-IR (KBr): 3330 cm⁻¹ (NH), 1855, 1732 cm⁻¹ (C=O, azetidine-2,4-dione), 1704 cm⁻¹ (C=O, urethane), 1650 cm⁻¹ (C=O, malonamide); ¹H NMR (DMSO-d₆): δ(ppm) = 0.79 (t, 3H, -CH₃), 1.17 (s, 30H, -CH₂), 1.33 (s, 18H, -CH₃), 1.54 (m, 2H, -CH₂), 2.3–2.36 (m, 12H, N-(CH₂-CH₂)₂-N-CH₂-), 3.17–3.39 (m, 12H, CONH-CH₂-CH₂), 3.73 (s, 4H, Ar-CH₂-Ar), 3.81 (s, 2H, Ar-CH₂-Ar), 3.98 (t, 2H, NHCOO-CH₂), 6.9–7.6 (m, 24H, Ar-H); Anal. Calcd for C₈₇H₁₁₆N₁₂O₁₀: Calcd. C, 70.13; H, 7.85; N, 11.28;

Found C, 69.55; H, 8.13; N, 10.90; MS: m/z (ESI) 1490 [M+]. GPC (THF): polydispersity = 1.00, M_w = 2807 g/mol, M_n = 2759 g/mol.

2.2.5. LG3.0

A solution of AEP (0.65 g, 5.04 mmol) in dry DMF (10 mL) was added slowly to a solution of LG2.5 (5 g, 3.36 mmol) in dry DMF (40 mL) under dry N_2 at 60 °C. After 6 h, all of LG2.5 had been consumed, the mixture was then poured into water (150 mL) and stirred for several minutes. The precipitate was purified through two cycles of dissolving in DMF and precipitating from water. Via drying under vacuum at 60 °C for 48 h, LG3.0 (4.9 g, 90%) was obtained as white powder. FT-IR (KBr): 3332 cm^{-1} (NH), 1704 cm^{-1} (C=O, urethane), 1640 cm^{-1} (C=O, malonamide); 1H NMR (Chloroform- d): δ (ppm) = 0.85 (t, 3H, -CH₃), 1.23 (s, 30H, -CH₂), 1.63 (s, 18H, -CH₃), 1.73 (t, 2H, -CH₂), 2.37–2.5 (m, 18H, NH-(CH₂-CH₂)₂-N-CH₂-), 2.81 (t, 4H, NH-(CH₂-CH₂)₂-), 3.37–3.39 (m, 14H, CH₂-CH₂-NHCO; N-(CH₂-CH₂)₂-N-CH₂-), 3.84 (s, 6H, Ar-CH₂-Ar), 4.1 (t, 2H, NHCOO-CH₂), 7–7.5 (m, 24H, Ar-H); Anal. Calcd for C₉₃H₁₃₁N₁₅O₁₀: Calcd. C, 68.99; H, 8.16; N, 12.98; Found C, 68.55; H, 8.14; N, 11.45; MS: m/z (ESI) 1619 [M+]. GPC (THF): polydispersity = 1.02, M_w = 2874 g/mol, M_n = 2811 g/mol.

2.2.6. LG3.5

A solution of IDD (1.48 g, 4.6 mmol) in dry THF (5 mL) was added slowly to a solution of LG3.0 (5 g, 3.1 mmol) in dry THF (45 mL) under dry N_2 at 60 °C. After 24 h, all of LG3.0 had been consumed. The solvent was evaporated and the product was purified through two cycles of dissolving in THF and precipitating from methanol. Via drying under vacuum at 60 °C for 48 h, LG3.5 (3.9 g, 65%) was obtained as white powder. FT-IR (KBr): 3338 cm^{-1} (NH), 1855, 1732 cm^{-1} (C=O, azetidine-2,4-dione), 1650 cm^{-1} (C=O, malonamide); 1H NMR (DMSO- d_6): δ (ppm) = 0.8 (t, 3H, -CH₃), 1.17 (s, 30H, -CH₂), 1.33 (s, 24H, -CH₃), 1.53 (m, 2H, -CH₂), 2.3–2.36 (m, 18H, N-(CH₂-CH₂)₂-N-CH₂-), 3.17–3.39 (m, 18H, CONH-CH₂-CH₂), 3.73 (s, 6H, Ar-CH₂-Ar), 3.81 (s, 2H, Ar-CH₂-Ar), 3.98 (t, 2H, NHCOO-CH₂), 6.9–7.5 (m, 32H, Ar-H); Anal. Calcd for C₁₁₂H₁₄₇N₁₇O₁₃: Calcd. C, 70.37; H, 7.73; N, 12.27; Found C, 69.73; H, 7.55; N, 11.75; MS: m/z (ESI) 1939 [M+]. GPC (THF): polydispersity = 1.03, M_w = 3097 g/mol, M_n = 3012 g/mol.

2.3. Synthesis of dendritic (A-DGs) and linear (A-LGs) pendants with primary amine

The general procedures for preparing poly(urea/malonamide) with primary amine (A-LGs and A-DGs) are described below (Schemes 1 and 2).

2.3.1. A-LG0.5

A dilute solution of LG0.5 (10 g, 16.9 mmol) in dry THF (500 mL) was added dropwise to a stirred solution of 1,4-aminobutane (14.9 g, 169 mmol) in dry THF (200 mL) at 0 °C. Reaction mixture was stirred for 3 h at room temperature and all of LG0.5 was consumed. The product was obtained by pouring the reaction solution into DI water, and the precipitate was collected. Via drying under vacuum at 60 °C for 48 h, A-LG0.5 (5.0 g, 50%) was obtained as light yellow powder. FT-IR (KBr): 3332 cm^{-1} (NH), 1704 (C=O, urethane), 1642 cm^{-1} (C=O, malonamide); 1H NMR (Chloroform- d): δ (ppm) = 0.86 (t, 3H, -CH₃), 1.23 (s, 30H, -CH₂), 1.43 (s, 6H, -CH₃), 1.64 (m, 6H, -CH₂), 1.93 (m, 2H, -CH₂), 3.32 (m, 2H, CONH-CH₂), 3.86 (s, 2H, Ar-CH₂-Ar), 4.13 (t, 2H, NHCOO-CH₂), 7.05–7.44 (m, 8H, Ar-H); Anal. Calcd for C₄₁H₆₆N₄O₄: Calcd. C, 72.53; H, 9.80; N, 8.25; O, 9.43; Found C, 72.39; H, 9.98; N, 8.13; MS: m/z (ESI) 679 [M+].

2.3.2. A-LG1.5

A dilute solution of LG1.5 (10 g, 9.62 mmol) in dry THF (500 mL)

was added dropwise into the stirring reaction at 0 °C to a solution of 1,4-aminobutane (8.48 g, 96.2 mmol) in dry THF (100 mL). Reaction mixture was stirred for 3 h at room temperature and all of the LG1.5 was consumed. The product was obtained by pouring the reaction solution into DI water, and the precipitate was collected. Via drying under vacuum at 60 °C for 48 h, A-LG1.5 (6.0 g, 55%) was obtained as light yellow powder. FT-IR (KBr): 3330 cm^{-1} (NH), 1704 cm^{-1} (C=O, urethane), 1642 cm^{-1} (C=O, malonamide); 1H NMR (Chloroform- d): δ (ppm) = 0.79 (t, 3H, -CH₃), 1.23 (s, 30H, -CH₂), 1.33 (s, 12H, -CH₃), 1.53 (m, 4H, -CH₂), 1.96 (m, 2H, -CH₂), 2.33–2.56 (m, 8H, N-(CH₂-CH₂)₂-N-CH₂-), 3.2–3.5 (m, 8H, CONH-CH₂-CH₂), 3.73 (s, 2H, Ar-CH₂-Ar), 3.81 (s, 2H, Ar-CH₂-Ar), 3.98 (t, 2H, NHCOO-CH₂), 7.01–7.56 (m, 16H, Ar-H); Anal. Calcd for C₆₆H₉₇N₉O₇: Calcd. C, 70.24; H, 8.66; N, 11.17; Found C, 68.94; H, 7.90; N, 12.03; MS: m/z (ESI) 1128.5 [M+].

2.3.3. A-LG2.5

A dilute solution of LG2.5 (10 g, 6.72 mmol) in dry THF (500 mL) was added dropwise to a stirred solution of 1,4-aminobutane (5.92 g, 67.2 mmol) in dry THF (100 mL) at 0 °C. Reaction mixture was stirred for 5 h at room temperature and all of the LG2.5 was consumed. The product was obtained by pouring the reaction solution into DI water, and the precipitate was collected. Via drying under vacuum at 60 °C for 48 h, A-LG2.5 (6.9 g, 55%) was obtained as light yellow powder. FT-IR (KBr): 3328 cm^{-1} (NH), 1704 cm^{-1} (C=O, urethane), 1642 cm^{-1} (C=O, malonamide); 1H NMR (Chloroform- d): δ (ppm) = 0.81 (t, 3H, -CH₃), 1.21 (s, 30H, -CH₂), 1.33 (s, 18H, -CH₃), 1.54 (m, 4H, -CH₂), 1.97 (m, 2H, -CH₂); 2.3–2.6 (m, 14H, N-(CH₂-CH₂)₂-N-CH₂-), 3.3–3.5 (m, 14H, CONH-CH₂-CH₂), 3.73 (s, 4H, Ar-CH₂-Ar), 3.81 (s, 2H, Ar-CH₂-Ar), 4.1 (t, 2H, NHCOO-CH₂), 6.9–7.5 (m, 24H, Ar-H); Anal. Calcd for C₉₁H₁₂₈N₁₄O₁₀: Calcd. C, 69.26; H, 8.18; N, 12.43; Found C, 68.74; H, 7.91; N, 13.23; MS: m/z (ESI) 1578 [M+].

2.3.4. A-LG3.5

A dilute solution of LG3.5 (10 g, 5.16 mmol) in 500 mL dry solvent [THF/DMF, 9:1 (v/v)] was added dropwise to a stirred solution of 1,4-aminobutane (4.54 g, 51.6 mmol) in dry THF (100 mL) at 0 °C. Reaction mixture was stirred for 5 h at room temperature and all of the LG2.5 was consumed. The product was obtained by pouring the reaction solution into DI water, and the precipitate was collected. Via drying under vacuum at 60 °C for 48 h, A-LG3.5 (7.8 g, 75%) was obtained as light yellow powder. FT-IR (KBr): 3328 cm^{-1} (NH), 1704 (C=O, urethane), 1642 cm^{-1} (C=O, malonamide); 1H NMR (DMSO- d_6): δ (ppm) = 0.8 (t, 3H, -CH₃), 1.17 (s, 30H, -CH₂), 1.33 (s, 24H, -CH₃), 1.54 (m, 4H, -CH₂), 1.97 (m, 2H, -CH₂), 2.2–2.4 (m, 20H, N-(CH₂-CH₂)₂-N-CH₂-), 3.17–3.39 (m, 20H, CONH-CH₂-CH₂), 3.73 (s, 6H, Ar-CH₂-Ar), 3.81 (s, 2H, Ar-CH₂-Ar), 3.98 (t, 2H, NHCOO-CH₂), 6.9–7.5 (m, 32H, Ar-H); Anal. Calcd for C₁₁₆H₁₅₉N₁₉O₁₃: Calcd. C, 68.71; H, 7.90; N, 13.13; Found C, 69.60; H, 7.82; N, 12.85; MS: m/z (ESI) 2008 [M+].

2.3.5. A-DG1.5

A dilute solution of DG1.5 (10 g, 6.23 mmol) in 500 mL dry solvent [THF/DMF, 9:1 (v/v)] was added dropwise to a stirred solution of 1,4-aminobutane (5.49 g, 62.3 mmol) in dry DMF (100 mL) at 0 °C. Reaction mixture was stirred for 3 h at room temperature and all of DG1.5 was consumed. The product was obtained by pouring the reaction solution into DI water, and the precipitate was collected. Via drying under vacuum at 60 °C for 48 h, A-DG1.5 (6.8 g, 65%) was obtained as light yellow powder. FT-IR (KBr): 3320 cm^{-1} (NH), 1704 cm^{-1} (C=O, urethane), 1642 cm^{-1} (C=O, malonamide); 1H NMR (DMSO- d_6): δ (ppm) = 0.79 (t, 6H, -CH₃), 1.23 (s, 60H, -CH₂), 1.33 (s, 18H, -CH₃), 1.53 (m, 8H, -CH₂), 1.94 (m, 2H, NH₂-CH₂-CH₂), 3.16 (m, 10H, CONH-CH₂-CH₂), 3.81 (s, 6H, Ar-CH₂-Ar), 3.98 (t, 4H,

NHCOO-CH₂), 7.98–7.56 (m, 24H, Ar-H); Anal. Calcd for C₁₀₁H₁₄₉N₁₁O₁₁: Calcd. C, 71.64; H, 8.87; N, 9.10; Found C, 71.01; H, 8.50; N, 8.93; MS: *m/z* (ESI) 1694 [M+].

2.3.6. A-DG2.5

A dilute solution of DG2.5 (10 g, 2.73 mmol) in 500 mL dry solvent [THF/DMF, 1:1 (v/v)] was added dropwise to a stirred solution of 1,4-aminobutane (2.41 g, 27.3 mmol) in dry DMF (100 mL) at 0 °C. Reaction mixture was stirred for 12 h at 60 °C and all of the DG1.5 was consumed. The product was obtained by pouring the reaction solution into DI water, and the precipitate was collected. Via drying under vacuum at 60 °C for 48 h, A-DG2.5 (8.1 g, 80%) was obtained as light yellow powder. FT-IR (KBr): 3340 cm⁻¹ (NH), 1704 cm⁻¹ (C=O, urethane), 1642 cm⁻¹ (C=O, malonamide); ¹H NMR (Chloroform-d): δ(ppm) = 0.85 (t, 12H, -CH₃), 1.23 (s, 120H, -CH₂), 1.39 (s, 36H, CH₃), 1.42 (s, 6H, CH₃), 1.60 (m, 12H, -CH₂), 1.97 (m, 2H, NH₂-CH₂-CH₂), 3.24 (m, 26H, CH₂(N)), 3.84 (s, 14H, Ar-CH₂-Ar), 4.12 (t, 8H, CH₂), 6.99–7.62 (m, 56H, Ar-H); Anal. Calcd for C₂₂₁H₃₁₅N₂₅O₂₅: Calcd. C, 71.32; H, 8.53; N, 9.41; Found C, 71.52; H, 9.05; N, 8.79; MS: *m/z* (MALDI-TOF) 3719 [M+].

2.4. Preparation of dendritic (DG-PU)s and linear (LG-PU)s side chain polyurethanes

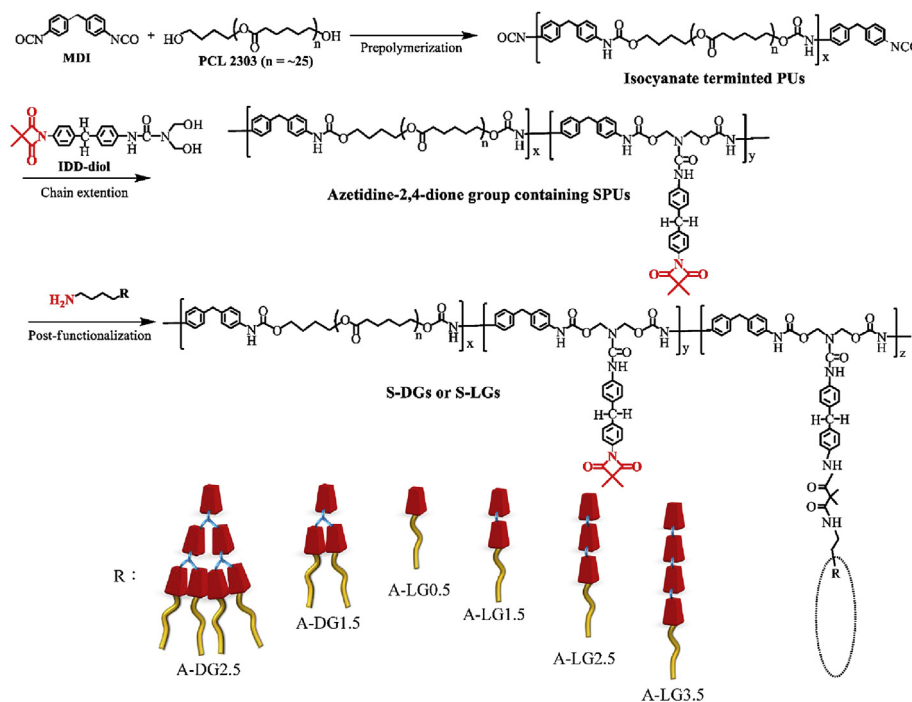
As shown in Scheme 3, azetidine-2,4-dione containing SPUs were synthesized according to procedures described in previous literature [39]. SPUs with different compositions were synthesized via a two-step condensation reaction. The reaction was carried out by adding MDI to a solution of PCL in 10 w/v % dry DMF. The reaction solution was heated at 60 °C for 0.5 h to obtain isocyanate terminated prepolymer by using di-n-butyltin dilaurate (T-12) as catalyst. Subsequently, the chain extender IDD-diols was added dropwise into the stirring reaction solution of isocyanate terminated prepolymer at 80 °C for 3 h to obtain azetidine-2,4-dione containing SPUs. The formulations of two SPUs (S35 and S45; designated Sxx, where xx is the HS content, wt.%) with different

contents of HS are summarized in Table 1. The weight-average molecular weights of S35 and S45 were 7.26×10^4 g/mol (PDI = 2.8) and 7.77×10^4 g/mol (PDI = 2.15), respectively.

SPUs with dendritic (Sxx-DGs; where xx is the HS content) and linear (Sxx-LGs) pendants were prepared by the post-functionalization of azetidine-2,4-dione group containing SPUs (S35 and S45) with different contents of amino group containing A-DGs and A-LGs (Scheme 3). SPU-DGs and SPU-LGs were obtained through the ring-opening reaction of azetidine-2,4-diones toward the aliphatic primary amine of A-DGs and A-LGs (designated Sxx-DGyy-zz and Sxx-LGyy-zz, where xx is the HS content, wt.%; yy is the generation of dendritic or linear pendant; zz is the content of pendant, mol.% to the azetidine-2,4-dione group content of SPU). A calculated amount of LG0.5, DG1.5, DG2.5, LG1.5, LG2.5 or LG3.5 dissolved in DMF was individually added to these SPU samples (S35 or S45) in DMF solution taken from the same batch and vigorously stirred at 80 °C for 12 h (Table S1 and Table S2). The reactions were monitored by a titration method described below for the amount of remaining azetidine-2,4-diones functional groups in the SPU sample. Therefore, a series of S-DGs (Sxx-DGyy-zz: xx = 35 and 45; yy = 0.5, 1.5, and 2.5; zz = 25, 50, 100) and S-LGs (Sxx-LGyy-zz: xx = 35 and 45; yy = 0.5, 1.5, and 2.5; zz = 25, 50, 100) were obtained. The as-polymerized solution was poured into Teflon circular disks at room temperature for 24 h and then heated to 60–70 °C for an additional 48 h. Thick films were obtained on the order of 270–300 μm thick.

2.5. Measurement

¹H NMR spectra were taken on a Bruker Avance-300 MHz FT-NMR spectrometer with chloroform-d and dimethyl sulfoxide-d₆. Elemental analysis was performed on a Heraeus CHN-OS Rapid Analyzer. Infrared spectra were recorded to identify the chemical structure of PUs using a Jasco 4100 FT-IR Spectrophotometer. Infrared spectra were measured with a Jasco ATR Pro 450-S accessory. Mass spectra were obtained using an electrospray



Scheme 3. Synthesis routes of PUs via post-functionalization method.

Table 1
Formulations, compositions, and HS contents of S35 and S45.

Samples	Composition (mole)				HS (wt %)	Mw*10 ⁴ (g/mol)	PDI
	MDI	PCL-3000	IDD-diol	Pendants			
S35	1.495	0.495	1	0	35.0	7.26	2.80
S45	1.307	0.307	1	0	45.0	7.77	2.15

ionization (ESI) source on a quadrupole ion trap mass spectrometer (Finnigan MAT LCQ classic, San Jose, CA, USA). Gel permeation chromatography (GPC) was performed using Viscotek viscoGEL (I-MBLMW-3078 and I-MBHMW-3078) columns and N-methyl-2-pyrrolidone (NMP) as the mobile phase. The samples were analyzed using a Shodex RI-101 GPC operated at a flow rate of 1.0 mL min⁻¹ at 40 °C with polystyrene calibration over the molecular weight range from 682 to 1670000 g mol⁻¹. Glass transition temperature (T_g), recrystallization temperature (T_c), and melting temperature (T_m) were measured under a N₂ atmosphere using a differential scanning calorimeter (DSC, TA Instruments, TA-Q20) operated at a heating rate of 10 °C min⁻¹. Degree of crystallinity of SS (X_{ms}) was calculated according to $(\Delta H_{ms}/\Delta H_{ms,100\%}) \times 100\%$, where $\Delta H_{ms,100\%}$ is the melting enthalpy of PCL (82.9 J/g). Thermogravimetric analysis (TGA) was performed under a N₂ atmosphere using a thermogravimetric analyzer operated at a heating rate of 10 °C min⁻¹ (TA Instruments, TGA-Q50). All samples were pre-heated at 105 °C for 30 min in the furnace to remove moisture.

Dynamic mechanical analysis (DMA) was performed using a PerkinElmer SII Diamond DMA instrument. The width and length of the strip PU specimens for mechanical tests were 5 and 20 mm, respectively. The values of storage moduli (E'), loss moduli (E'') and tan δ were determined for PU samples (thickness, 270–300 μm) that had been subjected to the temperature scan mode at a programmed heating rate of 2 °C/min under a N₂ atmosphere from -100 to 150 °C at a frequency of 1 Hz and an amplitude of 15 μm. Tensile strength measurements were carried out using a Gotech testing machine (AI-3000, Gotech Detection Device Co., Ltd., Taiwan) with a cross-head speed of 100 mm/min. Tensile specimens of SPUs were made according to ASTM D638 specification [40,41]. The tensile tester equipped with a temperature controlled chamber (GT-7001-HL) was also utilized to study the shape memory effect of the PU samples.

The conversion of reactive pendants, azetidine-2,4-dione function groups, in the SPU sample before and after post-functionalization were determined by a titration method. The procedure was similar to that of the titration of isocyanate as described in the literature [42]. PUs (0.1 g) was dissolved in 15 mL dry DMF for 15 min prior to addition of 5 mL solution of n-decylamine in dry DMF (0.1 N) and 5 drops of bromocresol green. The conversion % was calculated according to the following formula:

$$\text{Conversion\%} = (\text{B}-\text{V})_{\text{after}} / (\text{B}-\text{V})_{\text{before}}$$

where B and V are the required quantities of HCl for the end points of the blank (titration solution without PUs) and the testing sample, respectively.

Shape memory behavior was examined by cyclic thermo-mechanical tensile tests. The heating and cooling rate were controlled at 2 °C/min. The specimen was loaded to the strain (ε_m: 100%) at a constant crosshead speed of 10 mm/min at deformation temperature (T_{def}, 70 °C), that is 30 °C exceeding the melting temperature (T_{ms}) of SS based domains (Process 1). Subsequently, it was cooled to the fixing temperature (T_{fix}, 10 °C) under the same strain (Process 2) [43–45]. After 10 min, the load on the specimen was taken off (holding for 5 min), the fixed strain (ε_u) was recorded

(Process 3), then the specimen was heated from 10 °C to 70 °C, and the residual strain (ε_p) was recorded (Process 4). The shape fixity and shape recovery could be calculated based on the following equations:

$$\text{Shape retention ratio (\%)} = \epsilon_u / \epsilon_m \times 100.$$

$$\text{Shape recovery ratio (\%)} = (\epsilon_m - \epsilon_p) / \epsilon_m \times 100.$$

3. Results and discussion

3.1. Synthesis and characterization

The well-defined dendritic poly(urea/malonamide) pendants (LG0.5, DG1.0, DG1.5, DG2.0 and DG2.5) and their linear analogues (LG1.0, LG1.5, LG2.0, LG2.5, LG3.0 and LG3.5) were synthesized iteratively as shown in Schemes 1 and 2. For example, the highly reactive isocyanate unit of IDD was first reacted with stearyl alcohol to obtain LG0.5, which was then reacted with DETA to produce DG1.0. Subsequently, DG1.5 was obtained via the reaction between the isocyanate of IDD and secondary amine of DG1.0. Following the repetitive addition reaction of DETA and IDD, DG2.5 with seven units of (urea/malonamide) linkages was obtained. To prepare the linear analogues, the LG0.5 (i.e. LG0.5) was first reacted with AEP instead of DETA to produce compound LG1.0 as shown in Scheme 2. Subsequently, LG 1.5 was obtained via the reaction between the isocyanate of IDD and secondary amine of LG1.0. Following a similar repetitive procedure, linear polar pendant LG3.5 with four units of (urea/malonamide) linkages was obtained.

These poly(urea/malonamide) segments with various architectures were systematically prepared without the need of protection and deprotection steps. Via the repetitive addition reactions of active hydrogen based on the compound IDD as building block, these syntheses are efficient and straightforward reaction without side products in the absence of catalyst. It is important to note that linear poly(urea/malonamide) with more than four (urea/malonamide) linkages exhibited poor solubility in polar protic solvents such as DMF or DMAc due to the strong hydrogen bonding interactions from relatively close chain packing. On the contrary, the dendritic poly(urea/malonamide) with seven (urea/malonamide) segments is still soluble in organic solvent.

To ensure a more consistent polymer chain length, the hydrogen bond-rich pendants were incorporated onto PUs via post-functionalization. At first, the post-functionalizable SPUs (S35 and S45) were prepared by using IDD-diol as chain extender as shown in Scheme 3, and the formulation is listed in Table 1. The azetidine-2,4-dione functional group from IDD-diol could undergo facile ring-opening addition reactions with the aliphatic primary amine functional group, forming a malonamide linkage under mild condition [39]. For preparing poly(urea/malonamide) segments containing primary amine functional groups (A-LG0.5, A-LG1.5, A-LG2.5, A-LG3.5, A-DG1.5, and A-DG2.5), these DG and LG samples individually dissolved in organic solvents were poured into excessive amount of EDA solution. Consequently, a series of dendritic pendants (S35-DGs and S45-DGs) or linear analogues (S35-LGs and S45-LGs) grafted PUs were individually obtained by the addition reaction between azetidine-2,4-dione functional groups of SPUs (S35 or S45) and primary amine functional groups of functionalized poly(urea/malonamide) segments (Scheme 3, Table S1 and Table S2). This post-functionalization processes were terminated when more than 90 mole% of the azetidine-2,4-dione functional groups were consumed (monitored by the titration method). After post-functionalization, these PUs exhibited poor solubility once the solvent was removed due to the increased molecular weight as well

as strong hydrogen bonding interactions derived from the grafted polar pendants.

For the poly(urea/malonamide)s, the chemical structures of A-DGs, LGs, and A-LGs compounds were confirmed by FT-IR, ^1H NMR, elemental analysis, and mass spectra, and the characterization of DGs was reported in our previous work [32]. Fig. 1(a) shows the FTIR spectra of DG1.0, DG1.5 and A-DG1.5. The absorption peaks at 1650 cm^{-1} and 1704 cm^{-1} corresponding to the carbonyl group of the malonamide linkage was observed for DG1.0. Subsequently, the secondary amine of DG1.0 were reacted with IDD to produce DG1.5, leading to the emergence of absorption peaks at 1738 cm^{-1} and 1856 cm^{-1} from C=O stretching of azetidine-2,4-dione group. Moreover, the absorption peaks of azetidine-2,4-dione group was disappeared due to the ring opening reaction of primary amine from EDA to produce A-DG1.5. The absorption peak of N-H stretching from malonamide and urethane groups was observed at 3440 cm^{-1} for the DG1.0, DG1.5 and A-DG1.5. The FTIR spectra of the other dendritic pendants (LG0.5 and DG2.5) are similar to that of DG1.5, while amino group containing dendritic pendants (A-LG0.5 and A-DG2.5) are similar to that of A-DG1.5. Furthermore, the linear analogues of poly(urea/malonamide)s exhibited similar FTIR results. For example, the IR absorption characteristics of LG1.0, LG1.5 and A-LG1.5 are similar to those of the DG1.0, DG1.5 and A-DG1.5, accordingly as shown in Fig. 1(c). This is due to the fact that these dendritic and linear pendants possess similar structures of azetidine-2,4-diones, malonamides, and urethane groups but different architectures. On the other hand, ESI MS and MALDI-TOF MS were also employed for the determination of molecular weights of DGs and LGs (Table 2), which are in agreement with the calculated ones.

The chemical structure of PUs were confirmed by FTIR Spectroscopy as shown in Fig. 1(b) and (d). Before the post-

functionalization, the azetidine-2,4-dione group containing SPUs (S35 and S45) exhibited absorption peaks at 1743 cm^{-1} and 1855 cm^{-1} due to the presence of reactive azetidine-2,4-dione functional groups. After post-functionalization, the pendant grafted PUs exhibited a drastically decreased adsorption intensity of azetidine-2,4-diones because of the extensive addition reaction between azetidine-2,4-diones and primary amine functional groups of A-DG1.5 (Fig. 1(b)). The increasing intensity of adsorption peak at 1650 cm^{-1} and 1704 cm^{-1} indicates the formation of malonamide linkage for S45-DG1.5-25, S45-DG1.5-50 and S45-D1.5-100. Similar IR absorption characteristics were observed for LG grafted PUs as shown in Fig. 1(d).

3.2. Thermal properties

Thermogravimetric analysis (TGA) was carried out for the poly(urea/malonamide) segments (DG and LG pendants) as summarized in Table 2. All the pendants exhibit degradation temperatures T_d s higher than $200\text{ }^\circ\text{C}$. No weight loss was observed for these pendants within the operating temperature. Thermal phase behaviors of the poly(urea/malonamide) segments and the modified PUs were investigated using differential scanning calorimetry (DSC), operating at a heating and cooling rate of $5\text{ }^\circ\text{C}/\text{min}$ under nitrogen atmosphere, as discussed below.

Poly(urea/malonamide) segments. For the first heating runs of DGs and LGs as shown in Fig. 2, LG0.5 exhibited a distinct melting transition at $110\text{ }^\circ\text{C}$ without glass transitions due to the high degree of crystallinity. The rest of compounds (LG1.5, LG2.5, LG3.5, DG1.5 and DG2.5) show glass transition temperatures T_g at about $70\text{ }^\circ\text{C}$ as indicated by the arrows. Note that instead of the regular discontinuous curves for glass transition, the T_g s for the first runs here look like endothermic peaks. These hysteresis peaks for T_g should

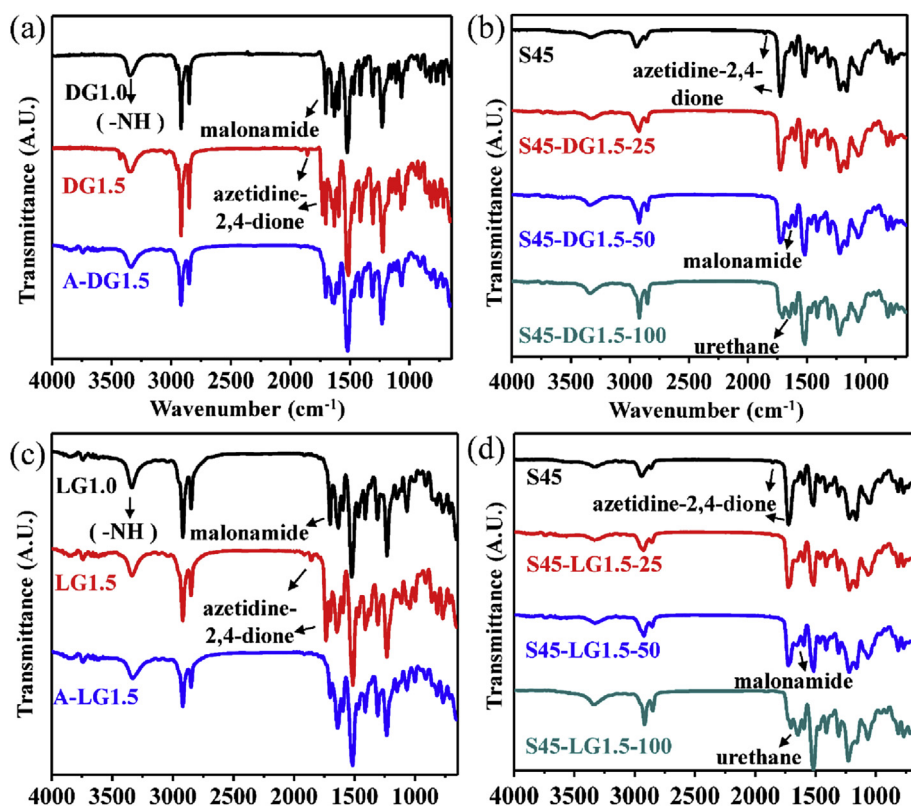


Fig. 1. FTIR spectra of (a) dendritic pendants (DG1.0, DG1.5, and A-DG1.5) and their PUs: (b) S45-DG1.5s containing various contents of DG1.5, and (c) linear pendants (LG1.0, LG1.5, and A-LG1.5) and their PUs: (d) S45-LG1.5s containing various contents of LG1.5.

Table 2
Characterization of dendritic(DGs) and linear(LGs) pendants.

Sample	Calcd. Mn	Mn ^a	Mw ^b	Mn ^b	PDI ^b	T _d ^c
DG0.5	591.8	591	1181	1164	1.01	272
DG1.0	1284.8	1284	–	–	–	250
DG1.5	1605.2	1605	4797	4608	1.02	277
DG2.0	3313.5	3313	8287	8044	1.03	271
DG2.5	3631.3	3632	9668	9392	1.03	278
LG0.5	591.8	591	1181	1164	1.01	272
LG1.0	720.0	720	1198	1152	1.01	204
LG1.5	1040.4	1040	1929	1893	1.01	252
LG2.0	1169.6	1169	2140	2117	1.01	214
LG2.5	1489.9	1490	2807	2759	1.00	253
LG3.0	1619.1	1619	2874	2811	1.02	226
LG3.5	1939.5	1939	3097	3012	1.03	252

^a Determined by ESI MS and MALDI-TOF MS.

^b Determined by GPC analysis in THF (calibration with polystyrene standards).

^c Degradation temperature (5% weight loss in N₂).

be associated with the relaxation of the residual chain orientation in the as-cast samples. At the second heating runs shown in Fig. S1, the hysteresis peaks disappear and turn to regular ones. Multiple melting peaks between 80 and 160 °C are observed for LGs or DGs with longer chains, indicating that varying crystal structures are formed by the different moieties on poly(urea/malonamide)s. For the second heating runs shown in Fig. S1, only LG0.5 can partially crystallize upon cooling at a rate of 5 °C/min while the crystallization of others are suppressed and only T_gs are detected at temperatures lower than those at first heating runs, indicating that the crystallization rates of long poly(urea/malonamide) are slow. The lower T_gs at second runs are due to less restriction from crystal phases against chain mobility in amorphous phases.

Soft-segment (SS) domains of PUs. Since PUs chains are composed of soft and hard segments arranging in an alternative manner, the properties of PUs strongly affected by the phase separation and the phase behaviors in each domain. The PU samples after synthesis were kept at room temperature and then cooled down to –60 °C. The first DSC heating scans for S35-DGs, S35-LGs, S45-DGs, and S45-LGs with 25 mol.% of pendant content are shown in Fig. 3 where several thermal transitions can be analyzed. A melting transition around 50 °C were associated to the crystalline phase of the SS domains mainly formed by the semi-crystalline PCL whose equilibrium melting point is around 60 °C [46]. At low temperatures, glass transitions of SS domain (T_{g,SS}) are not pronounced due to the high degree of crystallinity of PCL chains as well

as the diluted SS contents after the incorporation of the pendants. Only the samples with low HS contents such as S35 and S45 exhibited T_{g,SS} at about –40 °C for the molecular motion of PCL chains during the second heating runs in DSC measurements, where the crystallization of PUs are suppressed as shown in Figs. S2 and S3.

As mentioned in most of the literature on PUs, the crystallinity of SS are dependent on the HS contents. For the PUs with reactive side groups (S35 and S45) as shown in Fig. 3(a) and (b), they exhibited sharp endothermic melting peaks from the soft segments at 52 °C. The normalized degree of PCL crystallinity for S35 and S45 were high, 94.8% and 82.7%, respectively. This high degree of SS crystallinity may be caused by a more regular alignment of PCL chains in the SS domains that are phase separated from the HS domains in a well-defined manner. The phase separation process is less affected by the crystallization of HS due to the introduction of reactive pendants lowering the HS crystallinity [39], therefore resulting in distinct interfaces between domains that facilitate the alignments of PCL chains.

When LGs or DGs were incorporated onto the PU polymers as pendants, the HS fractions were increased and the SS was thus diluted. Furthermore, the steric effect of large pendants may hinder the packing of backbones, even for the PCL backbones in SS domains. Therefore, the PU samples with LGs or DGs as pendants exhibited a decrease in degree of SS crystallinity comparing to the pristine S35 and S45 as shown in the DSC curves. The total HS fractions of S35, S35-LG0.5-25, S35-LG1.5-25, S35-LG2.5-25 and S35-LG3.5-25 are 35.0, 39.5, 42.1, 45.0 and 46.8%, respectively. Their melting peaks of SS domains are at about 53 °C and the degree of crystallinity are 94.8%, 90.1%, 71.7%, 50.2%, and 3.3%, respectively, apparently decreased with increasing HS fraction. For the S45 grafted with LGs, the crystallinity decreases further and the melting transitions of SS domains even nearly disappear for those with linear pendants above 1.5 generations. The branching architecture of side groups also has a great impact on the crystallinity of SS domains. For example, both DG1.5 and LG2.5 have four units of urea/malonamide linkages and would cause similar total HS fraction. However, the S35-DG1.5-25 (X_m = 84.2%) shows a higher degree of crystallinity than S35-LG2.5-25 (X_m = 50.5%), as shown in Fig. 3(a). This result implies that the steric effect of the branched side groups may be less than that of linear side chains to hinder the close packing of SS backbones. The crystallization of all the crystallizable SS domains in PUs is greatly suppressed under a 5 °C/min cooling, as shown in the second heating runs in Fig. S3, indicating a slow crystallization rate for SS domains in all the PUs.

Hard-segment (HS) domains of PUs. For most of the PUs, multiple endothermic peaks are observed above 70 °C. Since this temperature is higher than the melting point of PCL (60 °C) in SS domains, these transitions should be rationally assigned to the melting of HS domains. Furthermore, the HS domains in S35 and S45 samples do not show melting peaks in this temperature range and therefore, the endothermic peaks above 70 °C must result exclusively from the grafted poly(urea/malonamide) pendants in HS domains [47].

Compared to the first heating runs of DSC data shown in Fig. 2, the melting temperatures of the HS domains in PUs at around 70 °C are mostly lower than those of corresponding poly(urea/malonamide)s. This endothermic peaks may include the glass transition followed by an orientation relaxation as discussed previously. Furthermore, endotherms at approximately 165 °C can be observed in the PU samples with dendritic pendants including S35-DG2.5-25, S45-DG1.5-25 and S45-DG2.5-25. These transitions are not observed for DG1.5 and DG2.5 (Fig. 2). The phase separation between SS and HS may be facilitated by the samples with longer HS (S45) and larger size of pendants (DG2.5), resulting in the main

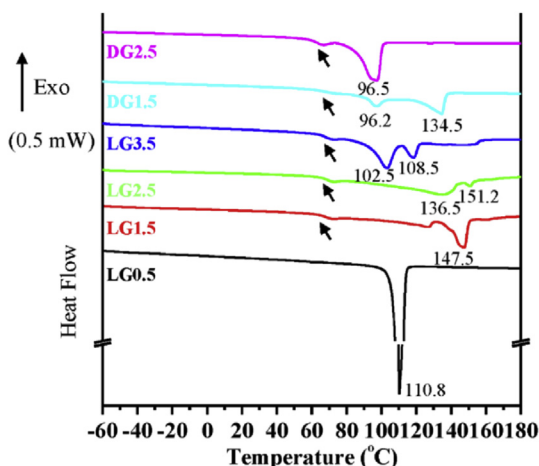


Fig. 2. DSC thermograms of DGs and LGs of the first heating scan.

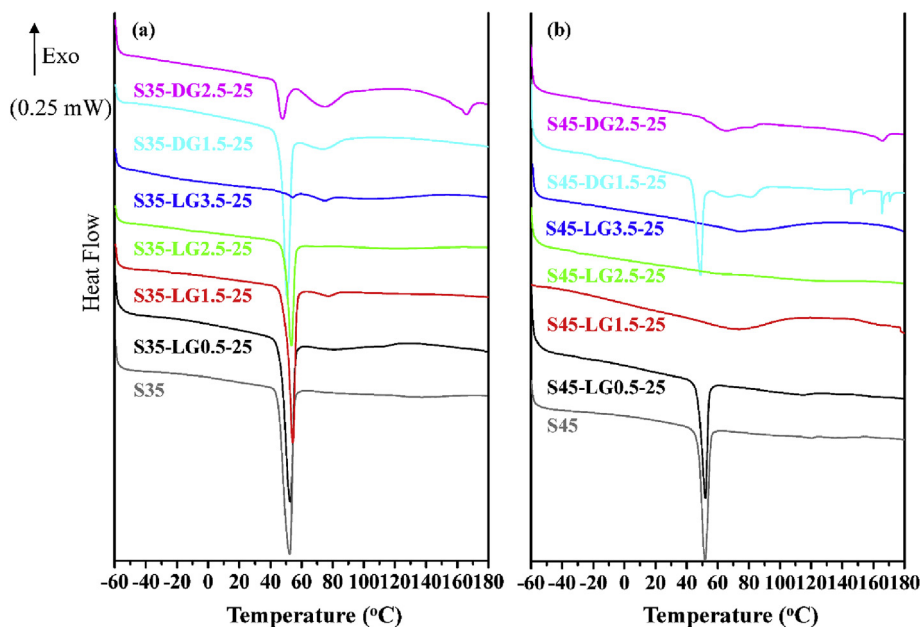


Fig. 3. DSC thermograms of the first PUs heating scan. (a) S35-DGs and S35-LGs with 25 mol.% of pendant content, and (b) S45-DGs and S45-LGs with 25 mol.% of pendant content.

chain crystallinity in HS domain [48]. For the samples with LGs as pendants, as the fraction of pendants increases, i.e. higher possibility of the pendants to reach one another, the crystallinity of the HS domains as well as the melting points are found to increase as shown in Fig. S2. This result indicates that the linear pendants are more readily for packing than DGs. Similarly, the crystallization rates of the pendants in HS domains are rather slow, which is evidenced by the second heating runs in DSC measurements where the melting peaks of the HS domains nearly disappear, as shown in Fig. S3.

3.3. Dynamic mechanical properties

The DMA curves of the S35-DGs, S35-LGs, S45-DGs, and S45-LGs with 25 mol.% of pendant content are presented in Fig. 4. The thermal mechanical properties are highly dependent on the glass transition and the melting. In comparison to the DSC data in Fig. 3, at the temperatures below 25 °C, the gradual decrease of the storage modulus E' with increasing temperature is attributed to the relaxation of amorphous SS domain, and around 60 °C, the sharp decrease of E' is mainly caused by the melting of crystalline SS domains. At temperatures higher than 60 °C, the transition is related to the melting or the breakdown of the HS domains.

Thermal mechanical properties are strongly dependent on HS contents for PU samples without pendants. Comparing the S35 and S45 samples, S45 shows a broader temperature range where the modulus is roughly constant above the glass transition of SS domains, i.e. rubbery plateau, than S35 does. The storage modulus of S35 is not detectable at temperatures higher than 80 °C, implying the sample disintegrates at a fairly low temperature. It appears that sufficient HS fractions are required to maintain a broad rubbery plateau with sufficient mechanical properties at high temperature, consistent with the result in previous report [39]. When polar pendants are incorporated into the PUs, it is not surprised that most of the samples show higher storage moduli due to the increased HS contents as shown in Fig. S4. Only the samples such as S35-LG2.5-25 and S35-LG3.5-25 have lower storage moduli than that of the pristine S35 below the melting transition of SS domains, possibly due to the lower degree of SS crystallinity.

In addition, thermal mechanical properties are more dependent on the architecture of pendants than on the HS contents for PU samples after post-functionalization. In Fig. S5 where the DMA curves are categorized into four groups with 45 ± 3 , 55 ± 3 , 65 ± 3 and 75 ± 3 wt% HS fractions, different characteristics of DMA curves can be clearly seen even when their HS contents are similar.

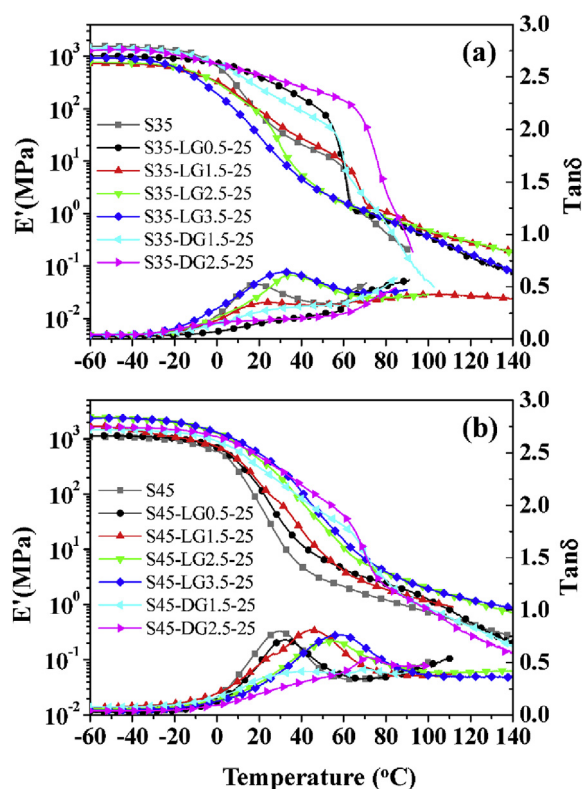


Fig. 4. Temperature dependence of the thermal mechanical properties at 1 Hz for PUs. (a) S35-DGs and S35-LGs with 25 mol.% of pendant content, and (b) S45-DGs and S45-LGs with 25 mol.% of pendant content.

For PUs with linear pendants, S35-LG2.5-25 and S45-LG2.5-25 exhibit more discernible SS melting relaxation, as indicated in the $\tan\delta$ curves. Meanwhile, these samples also possess broader rubbery plateau and higher moduli after the melting of SS domain. On the contrary, for most of the PUs grafted with DG1.5 or DG2.5, only a slight decrease of the storage modulus with increasing temperature was observed below the transition of HS domains. At the temperature range between 0 and 60 °C, the PUs samples grafted with DGs generally show higher storage moduli than those grafted with LGs (Fig. 4). When the temperature was increased, these PU samples quickly disintegrated after the melting of HS domains between 60 and 80 °C, indicating that the DG-grafted HS domains are less capable of serving as physical crosslinking junctions after melting.

For the PUs without significant crystallinity in both SS and HS domains, such as S45-LG2.5-25 and S45-LG3.5-25, a rather flat rubbery plateau above the glass transition of SS domains can be found. The HS domains would form stronger physical crosslinking interaction that can maintain the integrity of the samples at high temperatures. The samples with such a property can be easily deformed in the rubbery plateau regime and tend to recover to original states after the stress is released.

3.4. Mechanical properties

Stress-strain curves reveal the mechanical properties of S35-DGs, S35-LGs, S45-DGs, and S45-LGs with 25 mol.% of pendant content at room temperature as shown in Fig. 5. The S35 sample exhibits a semi-crystalline behavior with a yield stress, whereas the

S45 sample exhibits an elastomeric behavior with an elongation larger than 650%. This is because the crystallinity of SS domains in S35 is higher than that in S45 as shown in Fig. 3 and the SS domains dominate over the HS domains on the mechanical properties for S35 due to the much higher SS fraction.

For S35-LG samples, S35-LG0.5-25 show distinct yield stresses also because of the highly crystalline SS domains (Fig. 5(a)). The yield stress becomes obscure and lower as the total fraction of HS domains increases due to the lower crystallinity of SS domains. However, typical curves of semi-crystalline polymers reappear for the S35-LGs with 100% fraction of pendants, including S35-LG0.5-100, S35-LG1.5-100, and S35-LG2.5-100, which is attributed to the dominance of the crystalline HS domains in these samples as the total HS fraction are higher than 55% as shown in Figs. S6 and S7 [49]. Since the fraction of SS domains is low, the mechanical properties of S45-LGs are mainly regulated by the HS domains. As the total HS fraction increases, the yield stress increases too, but with smaller degree of elongation. Distinct yield stresses were observed for S45-LG1.5-25, S45-LG2.5-25, and S45-LG3.5-25 (Fig. 5(b)). In the cases of PUs with DG pendants, the stress-strain curves of both S35-DGs and S45-DGs are also determined by the HS domains. The yield stress increases with increasing length and fractions of the DG pendants as shown in Fig. 5 (a) and (b). The above results can be well correlated to the crystallization and phase behaviors in the thermal and dynamic mechanical tests.

3.5. Shape memory behavior

According to literature [45,50,51], SMPUs composed of polyesters such as PCL with switching temperatures at about 40 °C are suitable for clinical applications because of its closeness to the body temperature. To test the SMP performance, samples were programmed at 70 °C for deformation and 10 °C for fixation by using 40 °C as switching temperature as shown in Fig. 6. Although thermal transitions shifted to higher temperatures as shown in the result of $\tan\delta$ vs. temperature (Fig. 4), both S45-LG2.5-25 and S45-LG3.5-25 samples exhibited maximum thermal transitions ($\tan\delta$), and broad rubbery plateau in high moduli within the operating temperatures. Consequently, excellent shape memory behavior with shape recovery higher than 97% and shape fixity higher than 90% were achieved in the three round shape memory tests. On the other hand, the PUs grafted with DG1.5 or DG2.5 exhibited only a slight decrease of the storage modulus between 0 and 60 °C. When the temperature was further increased, the dendritic samples quickly disintegrated after the melting of HS domains between 60 and 80 °C, indicating that the DG-grafted HS domains are less capable of serving as physical crosslinking junctions after melting. Therefore, they are not fit for SMP materials.

4. Conclusion

In this study, PUs grafted with dendritic or linear poly(urea/malonamide)s of uniform chain lengths were synthesized via efficient and iterative syntheses. The consistency of polymer backbone confirmed by a titration analysis was achieved by the preparation of reactive PUs from one-pot reactor, followed by the post-functionalization methodology. The dynamic mechanical properties of the modified PUs were closely related to the architecture and length of polar pendants. Consequently, a variety of PUs elastomers could be achieved by tuning the architectures and the numbers of pendants. The results indicate that the PUs with linear pendants of more than four repeat units are capable of extending rubbery plateau, especially for those whose total fraction of hard segments close to 55 wt%. With the presence of a suitable phase transition and broad rubbery plateau, the linear polar pendants grafted PUs

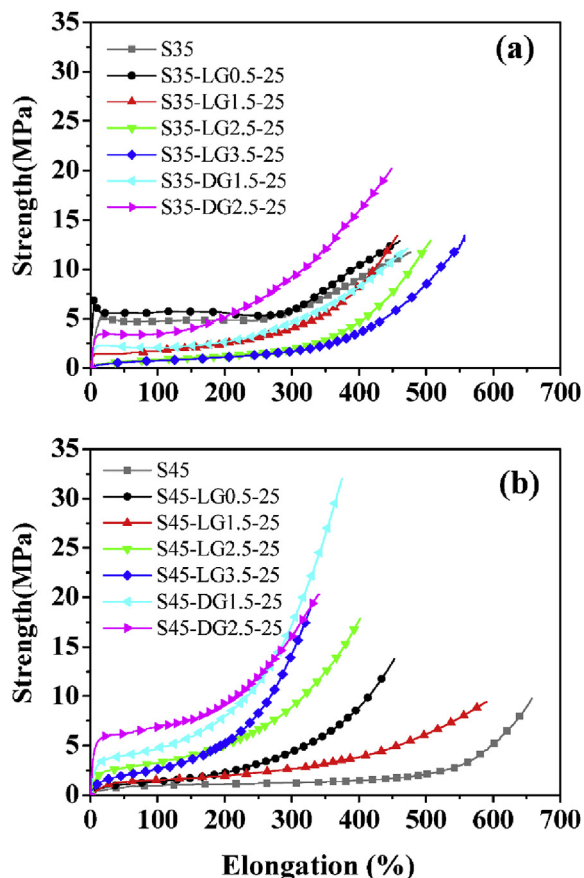


Fig. 5. Stress-strain curves of PUs. (a) S35-DGs and S35-LGs with 25 mol.% of pendant content, and (b) S45-DGs and S45-LGs with 25 mol.% of pendant content.

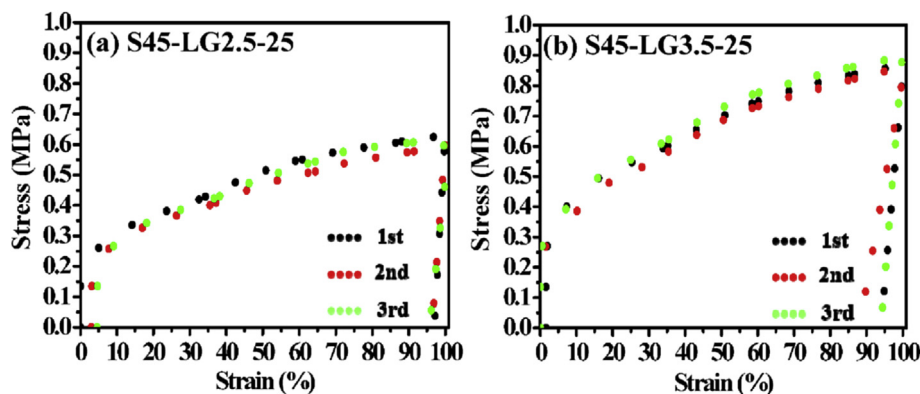


Fig. 6. Cyclic thermomechanical tensile tests revealed the thermal-induced shape memory behavior of (a) S45-LG2.5-25 and (b) S45-LG3.5-25. The samples were elongated to a strain of 100% at a stretching rate of 10 mm/min at 70 °C, and were then cooled down to 10 °C to maintain the deform state. The samples could return to the original shape after heating to 70 °C.

such S45-LG2.5-25 and S45-LG3.5-25 possess potential for making shape memory polymers.

Acknowledgments

We thank Ministry of Science and Technology of Taiwan (MOST 103-2221-E-002-277-MY2) and Chung-Shan Institute of Technology of Taiwan for financial support.

Appendix A. Supplementary data

Supplementary data related to this article can be found at <http://dx.doi.org/10.1016/j.polymer.2017.05.014>.

References

- [1] E. Delebecq, J.-P. Pascault, B. Boutevin, F. Ganachaud, On the versatility of urethane/urea bonds: reversibility, blocked isocyanate, and non-isocyanate polyurethane, *Chem. Rev.* 113 (1) (2013) 80–118.
- [2] L. Jiang, J. Wu, C. Nedolisa, A. Saiani, H.E. Assender, Phase separation and crystallization in high hard block content polyurethane thin films, *Macromolecules* 48 (15) (2015) 5358–5366.
- [3] P. Król, Synthesis methods, chemical structures and phase structures of linear polyurethanes. Properties and applications of linear polyurethanes in polyurethane elastomers, copolymers and ionomers, *Prog. Mater. Sci.* 52 (6) (2007) 915–1015.
- [4] Z.S. Petrović, J. Ferguson, Polyurethane elastomers, *Prog. Polym. Sci.* 16 (5) (1991) 695–836.
- [5] B. Lucio, J.L. de la Fuente, M.L. Cerrada, Characterization of phase structures of novel metallo-polyurethanes, *Macromol. Chem. Physic* 216 (20) (2015) 2048–2060.
- [6] Y.-C. Chung, N. Duy Khiem, B.C. Chun, Effects of the structures of end groups of pendant polydimethylsiloxane attached to a polyurethane copolymer on the low temperature toughness, *Polym. Eng. Sci.* 55 (8) (2015) 1931–1940.
- [7] Y.-C. Chung, H.Y. Kim, J.-H. Yu, B.C. Chun, Impact of cholesterol grafting on molecular interactions and low temperature flexibility of polyurethanes, *Macromol. Res.* 23 (4) (2015) 350–359.
- [8] S. Rimmer, M.H. George, Differential scanning calorimetry of some well defined poly(ϵ -caprolactone-*g*-PMMA)-co-polyurethanes, *Polymer* 35 (10) (1994) 2123–2127.
- [9] X. Wang, H. Li, X. Tang, F.-C. Chang, Syntheses and characterizations of soft-segment ionic polyurethanes, *J. Polym. Sci. Part B Polym. Phys.* 37 (8) (1999) 837–845.
- [10] S. Dassin, M. Dumon, F. Mechin, J.-p. Pascault, Thermoplastic polyurethanes (TPUs) with grafted organosilane moieties: a new way of improving thermomechanical behavior, *Polym. Eng. Sci.* 42 (8) (2002) 1724–1739.
- [11] Y.-C. Chung, I.-H. Jung, J.W. Choi, B.C. Chun, Characterization and proof testing of the halochromic shape memory polyurethane, *Polym. Bull.* 71 (5) (2014) 1153–1171.
- [12] Y.-C. Chung, J.W. Choi, H.Y. Kim, B.C. Chun, The effect of pendant tertiary butyl group on the shape recovery of polyurethane copolymer under freezing, *J. Elastomers Plastics* 45 (4) (2013) 333–349.
- [13] W. Yu, D. Zhang, M. Du, Q. Zheng, Role of graded length side chains up to 18 carbons in length on the damping behavior of polyurethane/epoxy interpenetrating polymer networks, *Eur. Polym. J.* 49 (6) (2013) 1731–1741.
- [14] Y.-C. Chung, J.W. Choi, D.H. Lee, B.C. Chun, The laterally attached tartaric acid of polyurethane copolymer and its impact on shape memory and low-temperature flexibility, *J. Intelligent Material Syst. Struct.* 23 (5) (2012) 505–513.
- [15] S. Randrasana, C.H. Baquey, B. Delmond, G. Daudé, C. Filliatre, Biocompatibility of Artificial Organs Polyurethanes grafted by pendent groups with different sizes and functionality, *Clin. Mater.* 15 (4) (1994) 287–292.
- [16] V. Bennevault, G. Richard, A. Deffieux, Polyurethane networks based on α,ω -dihydroxytelechelic and on random hydroxyl-functionalized side chain poly(2-chloroethyl vinyl ether): synthesis and investigation of mechanical properties, *Macromol. Chem. Physic* 198 (10) (1997) 3051–3064.
- [17] U.K. Stirna, I.V. Sevast'yanova, V.A. Yakushin, D.M. Vilsone, Synthesis and properties of comb-shaped segmented poly(urethanes) based on 1,2-propanediol derivatives, *Polym. Sci. Ser. B* 49 (11) (2007) 261–266.
- [18] K. Kojio, S. Nakamura, M. Furukawa, Effect of side groups of polymer glycol on microphase-separated structure and mechanical properties of polyurethane elastomers, *J. Polym. Sci. Part B Polym. Phys.* 46 (19) (2008) 2054–2063.
- [19] L. Zhang, M. Huang, R. Yu, J. Huang, X. Dong, R. Zhang, J. Zhu, Bio-based shape memory polyurethanes (Bio-SMPUs) with short side chains in the soft segment, *J. Mater. Chem. A* 2 (29) (2014) 11490–11498.
- [20] C.D. Eisenbach, T. Heinemann, Thermoplastic graft copolymer elastomers with chain-folding or bifurcated side chains, *Macromol. Chem. Physic* 196 (8) (1995) 2669–2686.
- [21] C.D. Eisenbach, T. Heinemann, A. Ribbe, E. Stadler, Chain architecture and molecular self-organization of polyurethanes: perspectives for thermoplastic elastomers, *Die Angew. Makromol. Chem.* 202 (1) (1992) 221–241.
- [22] C.D. Eisenbach, T. Heinemann, Synthesis and characterization of thermoplastic graft copolymer elastomers with a polyether main chain and uniform urethane-based side chains, *Macromolecules* 28 (7) (1995) 2133–2139.
- [23] N. Feuerbacher, F. Vögtle, Iterative Synthesis in Organic Chemistry, Dendrimers, Springer Berlin Heidelberg, Berlin, Heidelberg, 1998, pp. 1–18.
- [24] H. Noguchi, K. Hojo, M. Suginome, Boron-masking strategy for the selective synthesis of oligoarenes via iterative Suzuki–Miyaura coupling, *J. Am. Chem. Soc.* 129 (4) (2007) 758–759.
- [25] A.J. Boydston, Y. Yin, B.L. Pagenkopf, A controlled, iterative synthesis and the electronic properties of oligo([p-phenyleneethynylene]-alt-(2,5-siloleneethynylene))s, *J. Am. Chem. Soc.* 126 (33) (2004) 10350–10354.
- [26] C.-C. Tsai, T.-Y. Juang, S.A. Dai, T.-M. Wu, W.-C. Su, Y.-L. Liu, R.-J. Jeng, Synthesis and montmorillonite-intercalated behavior of dendritic surfactants, *J. Mater. Chem.* 16 (21) (2006) 2056–2063.
- [27] D.A. Tomalia, Birth of a new macromolecular architecture: dendrimers as quantized building blocks for nanoscale synthetic polymer chemistry, *Prog. Polym. Sci.* 30 (3–4) (2005) 294–324.
- [28] C.-P. Chen, S.A. Dai, H.-L. Chang, W.-C. Su, R.-J. Jeng, Facile approach to polyurea/malonamide dendrons via a selective ring-opening addition reaction of azetidine-2,4-dione, *J. Polym. Sci. Part A Polym. Chem.* 43 (3) (2005) 682–688.
- [29] S.A. Dai, T.-Y. Juang, C.-P. Chen, H.-Y. Chang, W.-J. Kuo, W.-C. Su, R.-J. Jeng, Synthesis of N-aryl azetidine-2,4-diones and polymalonamides prepared from selective ring-opening reactions, *J. Appl. Polym. Sci.* 103 (6) (2007) 3591–3599.
- [30] Y.-Y. Siao, S.-M. Shau, W.-H. Tsai, Y.-C. Chen, T.-H. Wu, J.-J. Lin, T.-M. Wu, R.-H. Lee, R.-J. Jeng, Orderly arranged NLO materials on exfoliated layered templates based on dendrons with alternating moieties at the periphery, *Polym. Chem.* 4 (9) (2013) 2747–2759.
- [31] Y.-Y. Hsu, S.-C. Yeh, S.-H. Lin, C.-T. Chen, S.-H. Tung, R.-J. Jeng, Dendrons with Urea/malonamide Linkages for Gate Insulators of n-channel Organic Thin Film Transistors, *Reactive and Functional Polymers*.
- [32] C.-P. Chen, S.A. Dai, H.-L. Chang, W.-C. Su, T.-M. Wu, R.-J. Jeng, Polyurethane elastomers through multi-hydrogen-bonded association of dendritic structures, *Polymer* 46 (25) (2005) 11849–11857.

- [33] S.A. Dai, C.-P. Chen, C.-C. Lin, C.-C. Chang, T.-M. Wu, W.-C. Su, H.-L. Chang, R.-J. Jeng, Novel side-chain dendritic polyurethanes based on hydrogen bonding rich polyurea/malonamide dendrons, *Macromol. Mater. Eng.* 291 (4) (2006) 395–404.
- [34] C.-C. Tsai, C.-C. Chang, C.-S. Yu, S.A. Dai, T.-M. Wu, W.-C. Su, C.-N. Chen, F.M.C. Chen, R.-J. Jeng, Side chain dendritic polyurethanes with shape-memory effect, *J. Mater. Chem.* 19 (44) (2009) 8484–8494.
- [35] M.-C. Kuo, R.-J. Jeng, W.-C. Su, S.A. Dai, Iterative synthesis of extenders of uniform chain lengths for making thermo-reversible polyurethane supramolecules, *Macromolecules* 41 (3) (2008) 682–690.
- [36] M.-C. Kuo, S.-M. Shau, J.-M. Su, R.-J. Jeng, T.-Y. Juang, S.A. Dai, Preparation of supramolecular extenders with precise chain lengths via iterative synthesis and their applications in polyurethane elastomers, *Macromolecules* 45 (13) (2012) 5358–5370.
- [37] C. Burger, W. Ruland, A.N. Semenov, Polydispersity effects on the microphase-separation transition in block copolymers, *Macromolecules* 23 (13) (1990) 3339–3346.
- [38] C. Burger, W. Ruland, A.N. Semenov, Polydispersity effects on the microphase-separation transition in block copolymers [Erratum to document cited in CA113(2):7140f], *Macromolecules* 24 (3) (1991) 816, 816.
- [39] C.-H. Wu, S.-M. Shau, S.-C. Liu, S.A. Dai, S.-C. Chen, R.-H. Lee, C.-F. Hsieh, R.-J. Jeng, Enhanced shape memory performance of polyurethanes via the incorporation of organic or inorganic networks, *Rsc Adv.* 5 (22) (2015) 16897–16910.
- [40] Y.-C. Chung, N. Khiem, J. Choi, B. Chun, Application of lateral sol–gel type crosslinking to a polyurethane copolymer, *J. Sol-Gel Sci. Technol.* 64 (3) (2012) 549–556.
- [41] B. Chun, M. Chong, Y.-C. Chung, Effect of glycerol cross-linking and hard segment content on the shape memory property of polyurethane block copolymer, *J. Mater. Sci.* 42 (16) (2007) 6524–6531.
- [42] S. Bonakdar, S.H. Emami, M.A. Shokrgozar, A. Farhadi, S.A.H. Ahmadi, A. Amanzadeh, Preparation and characterization of polyvinyl alcohol hydrogels crosslinked by biodegradable polyurethane for tissue engineering of cartilage, *Mater. Sci. Eng. C* 30 (4) (2010) 636–643.
- [43] J. Hu, Z. Yang, L. Yeung, F. Ji, Y. Liu, Crosslinked polyurethanes with shape memory properties, *Polym. Int.* 54 (5) (2005) 854–859.
- [44] K. Paderni, S. Pandini, S. Passera, F. Pilati, M. Toselli, M. Messori, Shape-memory polymer networks from sol–gel cross-linked alkoxyisilane-terminated poly(ϵ -caprolactone), *J. Mater. Sci.* 47 (10) (2012) 4354–4362.
- [45] L. Xue, S. Dai, Z. Li, Synthesis and characterization of three-arm poly(ϵ -caprolactone)-based poly(ester–urethanes) with shape-memory effect at body temperature, *Macromolecules* 42 (4) (2009) 964–972.
- [46] A. Sarasam, S.V. Madhally, Characterization of chitosan–polycaprolactone blends for tissue engineering applications, *Biomaterials* 26 (27) (2005) 5500–5508.
- [47] J.T. Koberstein, A.F. Galambos, Multiple melting in segmented polyurethane block copolymers, *Macromolecules* 25 (21) (1992) 5618–5624.
- [48] J.W.C. Van Bogart, P.E. Gibson, S.L. Cooper, Structure-property relationships in polycaprolactone-polyurethanes, *J. Polym. Sci. Polym. Phys. Ed.* 21 (1) (1983) 65–95.
- [49] B.K. Kim, Y.J. Shin, S.M. Cho, H.M. Jeong, Shape-memory behavior of segmented polyurethanes with an amorphous reversible phase: the effect of block length and content, *J. Polym. Sci. Part B Polym. Phys.* 38 (20) (2000) 2652–2657.
- [50] Y. Feng, M. Behl, S. Kelch, A. Lendlein, Biodegradable multiblock copolymers based on oligodepsipeptides with shape-memory properties, *Macromol. Biosci.* 9 (1) (2009) 45–54.
- [51] K. Kratz, U. Voigt, A. Lendlein, Temperature-memory effect of copolyesterurethanes and their application potential in minimally invasive medical technologies, *Adv. Funct. Mater.* 22 (14) (2012) 3057–3065.